Gold Recovery From Artificial Seawater Using Synthetic Materials And Seaweed Biomass To Induce Gold Nanoparticles Formation In Batch And Column Experiments

Pablo Lodeiro[1*] and Mika Sillanpää[2]

[1]*Department of Physical Chemistry and Chemical Engineering I, University of A Coruña, Rúa da Fraga 10, 15008 A Coruña, Spain.*

[2]*Laboratory of Green Chemistry, Department of Energy and Environmental Technology, Faculty of Technology, Lappeenranta University of Technology, Finland.*

*Corresponding author e-mail address: plodeiro@udc.es; Tel.: (+34) 981 167000 (ext. 2199); Fax: (+34) 981 167065

Abstract

Gold recovery from artificial seawater was studied in the present work. Two synthetic materials composed of silica gel joint to a strong chelating agent were used as reducing agents to induce gold colloid nanoparticles formation: ethylene diamine tetraacetic acid and diethylene triamine pentaacetic acid, together with brown seaweed *Sargassum muticum*. The mechanism and ideal conditions involving gold recovery from artificial seawater were investigated. The results showed that there is no pH effect within the range of 2-6. Moreover, the presence of other metals like Co, Ni, and Cr(VI) did not interfere the gold sorption/reduction reactions. Only thiourea showed significant regeneration percentages of the materials saturated with metallic gold. The absence of complete gold appearance in the effluent during column experiments could indicate that the sorption capacity of the materials was saturated, but not their reduction power. The shape of the obtained curves during the kinetic experiments revealed several stages occurring during the gold recovery from artificial seawater. Potentiometric titrations, FTIR, and SEM analysis provided decisive evidence supporting the proposed mechanism. A novel plausible three-step mechanism was suggested for the gold recovery from artificial seawater based on the experimental evidence. In a first stage, the adsorption of the anion species $AuCl_4^-$ occurred. Following, the reduction of $AuCl_4^-$ to Au(0), and the later oxidation of the metallic gold formed to the unstable $AuCl_2^-$ arose. Finally, during the last stage metallic gold redisolution is not further favored, and probably only the reduction of the chloro-gold complexes to metallic gold occurred.

Keywords: Precious metal; *Sargassum muticum*; EDTA; DTPA; silica gel; nanoparticle.

1. INTRODUCTION

Gold is a noble metal that has a high economic value, even more nowadays, due to its consideration as safe deposit in the times of economic recession. It also has several industrial and medical applications. The gold recovery from electronic waste, geological samples, ores or solution has been extensively studied during the last decades (Kavakli et al., 2006; Nilanjana, 2010; Syed, 2012).

To overcome the aggregation and stability problems that usually affect the metal nanoparticles in solution, normally a solid matrix to immobilize and reduce gold ions is employed. One of the most used methods to recover gold from solution consists of its reduction over the surface of an appropriate material, (Castro et al., 2011; Johnston and Lucas, 2011; Mata et al., 2009) or in the bulk of the solution, employing an extract obtained from materials of biological origin (Dubey et al., 2010; Montes et al., 2011). Moreover, some synthetic materials, including, silica or EDTA, also showed good complexation-reduction capabilities for gold ion (Choma et al., 2011; Sreeprasad and Pradeep, 2011).

These methods possess metal reduction ability, which leads to gold nanoparticles formation. The obtained gold nanoparticles show noticeable change in different physical and chemical properties such as electrical, catalytical, optical, etc. with respect to metallic gold. This also increases the inherent value of this study because of the multiple uses of gold nanoparticles in medicine, chemistry, biology, or material science (Guo and Wang, 2007; Saha et al., 2012).

To the best of our knowledge, there are no publications concerning gold recovery from seawater but a few patents (Layton and Mueller, 1981). Only several attempts have been carried out to recover gold from seawater since long time ago, but the huge troubles to approach it make these efforts useless, at least so far.

Gold is normally present in seawater in very low concentrations. An approximate average concentration value is in the order of ppt (Falkner and Edmond, 1990; Koide et al., 1988). More than 70% of the Earth's surface is covered by seawater, which represents 97% of the global water resources (2% is snow and glaciers and less than 1% fresh water), so the total quantity of gold is immense. Its recovery from seawater is not a simple task and presents a lot of difficulties and challenges. Firstly, the concentration of gold in seawater is very low, which implies that tones of seawater must be moved in order to recover a small amount of this precious metal. Secondly, the measurement of these very low concentrations in a not simple matrix solution with accuracy is difficult.

Because of the facts exposed above, the gold recovery from artificial seawater (ASW) spiked with this precious metal is studied in this work. The gold concentration in this artificial seawater solution is in the order of ppm. In this way, we can ensure accurate measurements for gold and deepen the understanding of the mechanism and factors that could affect the process.

Ethylene diamine tetraacetic acid (EDTA) and diethylene triamine pentaacetic acid (DTPA) are widely used sequestering agents for metal having several industrial applications (Rämö and Sillanpää, 2001; Rämö et al., 2000; Sillanpää, 1996; Sillanpää et al., 1995; Sillanpää and Pirkanniemi, 2001; Sillanpää and Sihvonen, 1997). The synthetic materials composed of silica gel joint to these strong chelating agents used in this work, namely EDSG and DTSG, were prepared before and tested with success for the elimination of different metals from solution (Repo et al., 2009). Here, the recovery of gold from artificial seawater is studied in continuous (columns) and discontinuous (batch) experiments. The efficiency of these materials for gold removal by nanoparticle formation was determined analyzing the influence of multiple factors such as the effect of pH, dose of material, contact time, or the presence of other metals (Co, Ni and Cr).

Co and Ni were selected because they were studied in a previous work using EDSG and DTSG materials (Repo et al., 2009). In that paper, it was demonstrated that Ni^{+2} and Co^{+2} are removed from solution due to due to columbic forces. On the contrary, Cr(VI) was selected because is presented in solution as negative specie, like Au, and it is normally removed from solution by a coupled sorption-reduction mechanism.

In addition, the brown seaweed *Sargassum muticum* was also tested under the best gold recovery conditions obtained with the synthetic materials. Dead macroalgae show high affinity for metal cations due to their high content in polysaccharides with acid functional groups (Herrero et al., 2011; Lodeiro et al., 2010). In brown algae, the cell wall is mainly comprised of alginates which usually constitute about 20-40% of the total dry weight, in addition to fucoidans (Davis et al., 2003). Moreover, biomass also possesses several groups, like hydroxyl or amine, with a great reduction capability, not only for precious metals but for contaminants like Cr(VI) (López-García et al., 2010).

2. EXPERIMENTAL SECTION

The metal solutions used in the experiments were prepared using the following salts: $HAuCl_4 \cdot 3H_2O$, CrO_3, $Co(NO_3)_2 \cdot 6H_2O$, and $Ni(NO_3)_2 \cdot 6H_2O$ (Sigma-Aldrich). It is worth to mention that these salt solutions were dissolved in artificial seawater (ASW) which was prepared following the recipe of Millero (Millero, 1986): NaCl (0.4117 mol/Kg), KCl (0.0102 mol/Kg), $CaCl_2$ (0.0104 mol/Kg), $MgCl_2$ (0.0532 mol/Kg), and Na_2SO_4 (0.0282 mol/Kg).

During batch experiments, the materials were put into contact with the metal solutions by magnetic agitation. Redox potential (E_{redox}) and pH were measured using a redox electrode (Thermo AD100) and a combined glass electrode (WTW pH-electrode SenTix 81meter), respectively.

Samples were taken periodically and measured for metal concentration as described below. The measurements of the samples were performed at least by triplicate. All the experiments were done at least two times and the results show the medium values obtained.

Materials

The chelating agents, EDTA and DTPA, were used to functionalize silica gel (LiChroPrep® Merck in powder form: diameter: 63–200 μm, surface area: 540 m^2/g) and to prepare the synthetic materials used in this work. The procedure to obtain these materials, namely EDSG and DTSG, was described by Repo *et al*. (Repo et al., 2009; Repo et al., 2011).

Fresh samples of brown marine alga *Sargassum muticum* were collected from the coast of A Coruña (NW Spain). The samples were washed first with running and then deionized water. Dried samples (oven-dried at 60 ºC overnight) were crushed with an analytical mill (IKA A 10) and sieved to a size range of 0.5-1 mm. After being sieved, the biomass was protonated in 0.1 M HNO_3 (10 g of biomass/L) for 4 hours at room temperature, washed with deionized water, filtered, and dried overnight at 60 ºC (Figueira et al., 2000).

Metal analysis

The samples were analyzed by an inductively coupled plasma optical atomic emission spectrometer (ICP-OES), model iCAP 6300 (Thermo Electron Corporation, USA). After filtering (0.45 μm acetate filter) and diluting with 2% HNO_3, the metal concentration in solution was measured at the following wavelengths: 242.7-267.5 nm for Au, 228.6 nm for Co, and 231.6 nm for Ni. The minimum detectable concentrations for Au, Cr, Co, and Ni ions by this equipment were 1.0, 1.1, 0.4, and 0.8 μg/L, respectively.

The metal removal percentages were calculated from the expression:

$$\text{Removal } \% = \frac{C_i - C_f}{C_i} \times 100 \quad (1)$$

where C_i is the initial metal concentration and C_f is the final metal concentration.

Effect of dosage

10 mL of gold solution (0.25 mM) was added to different essay tubes containing 1, 5, 10, 20, and 40 mg of EDSG and DTSG. Gold concentration in solution was measured after 27 and 161 hours of contact time.

Effect of pH

10 mL of Au solutions (0.5 mM) was placed in different essay tubes containing 40 mg of EDSG, DTSG, or protonated *Sargassum muticum*. The solution pH was adjusted to values between 2 and 6 using HNO_3 or NaOH (Merck). Gold concentration in solution was measured after 24 and 168 hours of contact time.

Kinetic studies

The experiments were carried out in sealed glass cells. 400 mg of the materials (EDSG, DTSG, or protonated *S. muticum*) were added to 100 mL of Au solution (0.05, 0.25, and 0.5 mM).

Regeneration studies

Regeneration studies were carried out using thiourea 0.5 M in HCl 1 M as desorbing agent. The materials, EDSG and DTSG, were previously saturated with Au in experiments conducted at fixed pH (3.0) and metal concentration (0.5 mM). When equilibrium was achieved, the solution was filtered and the material was dried in an oven at 60 ºC overnight. This material was placed in essay tubes together with the regeneration agent (4 g/L) during 24 and 120 hours.

Effect of metal competition

The competition effect of Cr, Ni, and Co ions over gold recovery was tested through batch sorption experiments carried out using 40 mg of DTSG. The material was contacted with 10 mL of gold solutions (0.5 mM) and the competitor metal ion at three different initial concentrations (0.05, 0.5, and 5.0 mM) during 96 hours.

Column studies

The experiments were carried out in plastic columns with 10-cm length and 0.5-cm internal diameter filled with different quantities of EDSG (0.05, 0.1, and 0.2 g). A 0.005 mM Au solution was fed through the column in down-flow mode using a Watson Marlow peristaltic pump. This solution was prepared from a gold standard solution (Au in HNO_3, Sigma-Aldrich) of 1000 mg/L dissolved in artificial seawater. Two different flow rates were tested: 1 and 5 mL/min. The operation of the column was stopped when the gold concentration in the effluent remained constant.

Characterization of the materials

Potentiometric titrations

The potentiometric titrations were carried out in a thermostated double-walled beaker under a N_2 stream. The ionic strength of the solutions was fixed to 0.05 M using $NaNO_3$ as supporting electrolyte. 0.25 g of EDSG and DTSG were added to 25 mL of $NaNO_3$ containing 20 mL of NaOH 0.05 M (in order to ensure that all the groups were deprotonated). After the solution achieved equilibrium (16-20 hours), the titration was started adding a standardized HCl 0.05 M solution step by step using the Microlab 500 series equipment. The procedures that followed the titrations and glass electrode calibrations are described in greater detail elsewhere (Rey-Castro et al., 2004; Rey-Castro et al., 2003).

FTIR analysis

FTIR spectroscopy was used for the qualitative identification of the chemical groups present in the materials. In these experiments, EDSG, DTSG, and *S. muticum* were used before and after the kinetic studies (initial gold concentration of 0.5 mM). Moreover, the materials saturated with Au, Cr, Ni, and Co, as described in the *Effect of metal competition* section, were also tested. The samples were examined within the range 350–4000 cm^{-1} using a Bruker Vertex 70 spectrophotometer equipped with a Speac Golden Gate ATR (attenuated total reflection) device. This technique allowed the analysis of the samples (fine powder) directly without KBr grinding.

SEM analysis

Surface morphology of the adsorbents was characterized by scanning electron microscope (SEM) analysis, recorded on a JEOL JSM 6400 SEM equipped with an Oxford Inca Energy 200 system for Energy Dispersive X-ray Spectroscopy (EDS). The examinations were carried out at different magnifications (from 45 to 6000×) at a 20 kV acceleration voltage. These analyses were carried out over the same materials used for FTIR.

3. RESULTS AND DISCUSSION

Effect of dosage

Different dosages of EDSG and DTSG materials were tested in order to determine the optimal dose rate to be used during experiments. Table 1 shows the removal percentages of gold from ASW solution at different times and doses of materials.

The percentages of gold removal close to 100 % were obtained using a dose greater than 0.5 g/L. An optimal dose of 4 g/L was chosen to carry out further experiments, but great differences were not found between 2 and 4 g/L. The measured equilibrium pH values were between 3.10-3.73.

Effect of pH

The effect of pH over gold elimination from ASW solutions is showed in Figure S1. When the contact time was long enough, percentages of gold removal around 100% were achieved for all the materials in a pH range between 2 and 6. In the case of protonated *S. muticum*, final equilibrium values for a pH greater than 4 were not obtained. Initial pH values were fixed to values between 2 and 10, but the final equilibrium values were never greater than 4, even when the solution pH was adjusted several times during the experiments. The alga acts as a buffer in solution because of its resistance against pH changes when acid or base was added to the solution. Initial pH values between 4.5-10 lead to final pH values around 3.5-4.2 after several attempts to obtain final pH values greater than 4 adding different amounts of NaOH. Probably, the chemical groups present in this macroalga act as buffer stabilizing the pH of the solution.

The reduction capacity of the materials is maintained within a large range of pH (from 2 to 4-6). The medium pH value for real seawater is between 7.5 and 8.4, so a preceding acidification step is needed in order to apply this method for the recovery of gold present in real seawater.

The effect of pH is normally associated with the ionization state of the functional groups present in the materials and also to the metal speciation in the solution. The predominant gold compounds found using the Hydra-Medusa program (Puigdomenech, 1999) for speciation calculations are $AuCl_4^-$, $AuCl_3OH^-$, and $Au(OH)_3$ (Figure S2). In these calculations, the formation of the solid species $Au(OH)_3(s)$ was not considered since evidence of its appearance was not found during the experiments.

The lack of pH dependence on gold removal observed in Figure S1 is related to the fact that in the studied pH range, the amine and hydroxyl groups present in the materials are protonated (see section 3.7.1). This favors the electrostatic interactions with the anionic

chloro-gold complexes that are present in solution at pH values lower than 5. From this pH, the presence of the neutral species $Au(OH)_3$ starts to increase in ASW solution, being predominant from pH 5.5. As Au(III) is considered as a soft ion, the gold removal from ASW at pH values above 5.5-6 could involve the formation of covalent bounds between sulphur or nitrogen and the predominant neutral gold species, leading to different mechanisms of reduction. Moreover, the interactions with the charged carboxylate ions should also be considered, as previously described for mercury neutral species removal by macroalga (Carro et al., 2010).

Kinetic studies

Kinetic studies were carried out in order to determine the necessary time to achieve equilibrium. Figures 1, 2, and 3 show the gold concentration change with time in artificial seawater after contact with EDSG, DTSG, and protonated *S. muticum*, respectively.

The shape of these kinetic curves reveals several steps occurring during the gold recovery in ASW. For the initial gold concentration of 0.5 mM, recovery percentages around 95 % were obtained after 300, 380, and 1500 minutes for DTSG, EDSG, and protonated *S. muticum*, respectively.

When the initial gold concentration was 0.5 mM, a removal percentage around 65% was observed in the first minutes for DTSG and 50% for the other materials. Next, an increase in the metal concentration was observed up to 40 minutes with a gold removal percentage of 34 % for DTSG, and until 120 minutes with a removal percentage of 40% for EDSG and the algae. The last step consists of a diminution of gold concentration up to values around 100% of metal recovery.

When the initial gold concentration is lower than 0.5 mM, the first step of the kinetic mentioned above is missed. After the first gold removal, an increase can be observed in

this metal concentration during 60 minutes (DTSG) or 540 minutes (EDSG). Then, as for the higher initial gold concentration, a classical diminution in Au concentration was observed until it totally disappears from ASW solution.

This unusual kinetic behavior is probably due to the dissolution of some metallic gold formed after the $AuCl_4^-$ reduction during the first steps of the kinetic (Marsden and House, 2006). This process is known to be favored in high concentrated chloride solutions, like the ASW used in this work, with a chloride concentration of 0.51 M. In fact, when gold was recovered from aqueous solution, classical kinetic curves were obtained (not shown here, work under preparation).

Three different stages can be observed during the kinetic studies in ASW:

In the first stage, the adsorption of the $AuCl_4^-$ occurs, producing the observed gold concentration diminution in the ASW. This step was not detected when the gold initial concentration was lower than 0.5 mM because of the faster kinetic of adsorption.

During the second stage, an increase in the gold concentration was observed. The reduction of $AuCl_4^-$ to Au(0) and the later oxidation of the metallic gold formed to the unstable $AuCl_2^-$ occurred during this step. This species, which appears as a secondary intermediate, can be oxidized to $AuCl_4^-$, bind to some site in the materials or stay in solution. Then, it is possible that some gold was released back into the solution, producing the observed increase in the metal concentration. The confirmation of the beginning of the reduction was also achieved by the observation of a color change from yellow to dark brown in the surface of the materials at the end of this stage (100, 50, and 75 minutes for Au 0.5 mM removal using EDSG, DTSG, and *S. muticum*, respectively).

The third stage represents the classical kinetic curve decay. In this case, metallic gold redisolution is not further favored, and probably only the reduction of $AuCl_4^-$ to Au(0), the most thermodynamically favorable process, takes place.

The insets of the Figures 1, 2, and 3 show the variations of pH and redox potential during the kinetics of $HAuCl_4$ 0.5 mM. The tendency of these curves is very similar to the obtained for the change in gold concentration. Three stages were also observed coinciding with those described above. During the adsorption of the chloro-gold complex, the pH diminished and the redox potential increased. The opposite tendency was observed for the pH in the second stage, while the redox potential remained almost constant when elemental gold was oxidized to $AuCl_2^-$. This is in concordance with the mechanism proposed (see section 4). Finally, during the last step, a decrease of the pH and redox potential in ASW was found, according to the global reduction reaction for $AuCl_4^-$.

Regeneration studies

0.04 g of EDSG and DTSG, previously saturated with Au, were put into contact with 10 mL of thiourea 0.5 M containing HCl 1M. This desorbing agent was able to recover 73 and 78% of Au, previously retained in EDSG, after 24 and 120 hours of contact time, respectively. In the case of DTSG, the percentages of gold recovery were 73 and 82% for the same time periods. In acidic solution, the $SC(NH_2)_2$ compound is able to complex the metallic gold deposited on the surface of the materials and form the cationic species $Au[SC(NH_2)_2]_2^+$ which was dissolved in solution.

Significant desorption percentages were not obtained using other compounds such as HCl or NaOH. This is in concordance with the fact that the ion-exchange mechanism does not play a substantial role in the gold recovery process.

Effect of metal competition

Figures 4 and 5 show the effect of the presence of Ni, Co, and Cr(VI) at the initial concentrations of 0.05, 0.5, and 5 mM on gold recovery (0.5 mM) in artificial seawater using DTSG.

The pH values in solution varied between 2.6 and 3.2, depending on the metal concentrations. Contact time was 48 hours, and a dose of material of 4 g/L was used.

It seems that there is no effect over Au recovery due to the presence of these metals in artificial seawater solution. Gold removal percentages around 100 % were always attained, indicating that Cr(VI), Co and, Ni do not interfere the gold sorption/reduction reactions.

Speciation studies demonstrated that Co appears in gold-ASW solution mainly as cationic species: 50-55 % Co^{+2}, 20-25 % $CoCl^{+}$, and around 20 % CoSO4. In the case of Ni, the species distribution is the following: 45 % $NiCl_2$, 10% $NiSO_4$, 25 % $NiCl^{+}$, and 20 % Ni^{+2}. A previous study demonstrated that in aqueous solutions Ni and Co are adsorbed on the surface of EDSG and DTSG due to columbic forces between the positive charges of these metals (present in solution as Ni^{+2} and Co^{+2}) and the negative charge of the groups present in the materials (Repo et al., 2009). In this case, not only positive species are present, and the interactions with EDSG and DTSG can also be associated to neutral species. The results for Co and Ni removal in the presence of Au 0.5 mM in ASW are similar to the ones obtained before in the absence of gold and in aqueous solution (not identical conditions). Thus, it can be concluded that neither gold nor the high ionic strength due to ASW ions content affects significantly the Co and Ni elimination.

On the contrary, Cr(VI) appears in gold-ASW solution as an anionic species ($HCrO_4^{-}$). For the highest initial Cr(VI) concentration, speciation calculations also found a percentage of 23 % of $Cr_2O_7^{-2}$. In this case, it is expected that the mechanism for the

removal of this species is similar to the proposed for the gold anion complex. Nevertheless, there is no effect over gold removal, as stated before (Figure 5). The fact that gold was preferentially eliminated by DTSG can be justified based on the higher redox potential value for the gold reduction reaction, making this process more favorable.

Column studies

Columns studies were carried out using different quantities of EDSG (0.05, 0.1, and 0.2 g) at two flow rates: 1 and 5 mL/min (Figure 6).

The initial gold concentration was 0.005 mM prepared from gold ICP standard in ASW. As shown in Figure 6, in all experiments, gold appeared in the effluent solution in the very beginning, so classical breakthrough curves were not obtained. As it was shown above, the elevated ionic strength of the artificial seawater makes the adsorption/reduction of gold a slow process. The screening of the electrostatic charge in the materials due to the presence of high quantities of light metals (Na, Ca, K, and Mg), and also the steric impediments associated, inhibiting the approximation of Au to the reduction groups are slowing down the process. Then, the retention time inside the columns is not long enough to provide an adequate contact time for the complete gold removal to occur.

Using a fixed flow rate of 5 mL/min and varying the mass of EDSG inside the column, the gold concentration in the outlet decreased after 5 minutes in the following order: 0.0043, 0.0037, and 0.0035 mM for 0.05, 0.1, and 0.2 g of EDSG, respectively. As expected, the mass of the gold recovered from the ASW solution until the experiments were stopped increased with the mass of EDSG: 0.0065, 0.34, and 0.61 mg of Au for 0.05, 0.1, and 0.2 g of EDSG.

When the flow rate was diminished to 1 mL/min, the retention time inside the column increased. As a consequence, the quantities of gold retained in the material were considerably improved: 1.0, 1.1, and 2.3 mg of Au for 0.05, 0.1, and 0.2 g of EDSG. In a similar manner, the gold concentration found in the effluent after 5 minutes was lower with respect to the values found at a flow rate of 5 mL/min: 0.0024, 0.0022, and 0.002 mM for 0.05, 0.1, and 0.2 g of EDSG.

Speciation studies demonstrated that Au(I) is present in ASW as $AuClOH^-$. In this case, adsorption of this gold complex followed by its direct reduction to metallic gold is expected.

An additional confirmation of the reduction of gold was obtained from these column experiments. At the lowest flow rate, when there was more contact time between the solution and the material, the gold concentration in the effluent remained constant attaining less than 20 % of its initial concentration. This is an indication that not only the $AuClOH^-$ adsorption in the EDSG sites but also gold reduction occurred. The absence of complete metal appearance in the effluent could indicate that the sorption capacity of EDSG is saturated, but not its reduction power.

Characterization of the materials

Potentiometric titrations

The chemical groups present in these materials play a key role in the gold recovery from solution. The potentiometric titration studies allow the quantifying and identifying of these groups.

After several previous tests, the titrations of EDSG and DTSG were carried out in the following way: the material was added to 25 mL of $NaNO_3$ containing 5-20 mL of NaOH (in order to ensure that all the groups were deprotonated). Then, the solution was

allowed to achieve equilibrium (16-20 hours), before starting to titrate adding HCl step by step. When one of these experiments was finished, the inverse titration was also carried out. So, a new titration using NaOH was done over the same material previously titrated with HCl.

No hysteric behavior was detected between the direct and inverse titration (identical titration curves using acid or base as titrants over the same material, graph not shown), indicating the absence of hidden groups.

The titrations were carried out adding acid. Thus, before the start, the material was deprotonated, and the added acid was bounded step by step to the groups. We ensured the achievement of equilibrium between the material and basic solution, leaving them enough time to contact before starting the titration. The materials are not stable at very basic pH, so when we leave them in solution for a long time, they lose their structural properties. It seems that the acid groups are more accessible for protons operating in this way.

Using simple models like Katchalsky's equation (Katchalsky et al., 1954), potentiometric curves of a polyacid can be described considering the presence of only one type of chemical groups. However, if we consider that more than one type of acid groups is present in the materials, a different model has to be applied.

The proton dissociation of an acid group in the materials can be represented by the following reaction:

$$AH \leftrightarrow A^- + H^+ \quad (2)$$

The conditional dissociation constant for equation 2, K_H, can be defined as:

$$K_H = \frac{[A^-][H^+]}{[AH]} \quad (3)$$

From this equation, defining $[A_{tot}]$ as the total number of acid groups: the sum of protonated, [AH], and ionized groups, $[A^-]$, it is easy to obtain the following expression used to describe the potentiometric curves:

$$\sum_{j=1}^{N}[A_j^-] = \sum_{j=1}^{N}\frac{[A_{tot}]_j}{1+\frac{[H^-]}{K_{H,j}}} = \sum_{j=1}^{N}\frac{h_j}{1+\frac{[H^+]}{K_{H,j}}} \quad (4)$$

where h_j is the amount of specific acid groups (mol/L). The value for the ionized acid groups $[A_j^-]$ was calculated from the balance of electroneutrality:

$$\sum_{1}^{2}[A^-] = \left([H^+] + \frac{(V_{i,NaOH}[NaOH] - V_{HCl}[HCl])}{(V_0 + V_{HCl} + V_{i,NaOH})} - \frac{K_w}{[H^+]}\right)\frac{(V_0 + V_{HCl} + V_{i,NaOH})}{V_0} \quad (5)$$

where $V_{i,NaOH}$ is the volume of base added before the titration started (mL), V_0 is the initial volume of the neutral electrolyte addition (mL), and K_w is the ionic product of water.

The quantity of specific acid groups (h_j) and the conditional equilibrium constants ($K_{H,j}$) referring to $NaNO_3$ 0.05 M were obtained by fitting Equation 4 to every potentiometric curve, considering the presence of one, two, or three functional groups (Figure S3 and Table 2). The use of more than three acid groups was not taken into account due to the possible overparametization in the model.

The pK values for EDTA obtained from bibliography (Smith et al., 2007) are 0, 1.5, 2.0, and 2.69 (carboxylic acids); and 6.13 and 10.37 (amino groups). Similar values were also proposed for DTPA: 0.1, 0.7, 1.6, 2.0, and 2.7 (carboxylic acids); and 4.28, 8.6, and 10.5 (amino groups). In the materials used, one of the carboxylic groups reacted with an amino group obtained by silanization with the silica gel, obtaining the final EDSG or DTSG materials that contain an amide group which was not initially present. The pK value for this amide group is around 15, and it will be always protonated during the titration experiments.

The minimum pH value achieved during titration experiments was 2.5. Taking into account the pK values showed above, almost all the carboxylic groups were not protonated during titration, so they cannot be quantified.

As can be seen in Figure S3, the consideration of only one acid group in Equation 4 was not able to describe both titration curves. However, it is difficult to choose between the models with two or three groups based on the goodness of fit, as both describe the potentiometric curves accurately. Moreover, the loss of the structural properties of the materials at basic pH could produce the break of some bounds and generate the appearance of some groups initially present in the precursors of the EDSG and DTSG materials.

If the presence of only two main groups is considered in the case of EDSG, the amount of the functionalities obtained is 2.2 and 0.34 mmol/g (Table 2). These groups can be attributed to amino groups (pK_H= 10.04 and 4.9, respectively), but hydroxyl entities, coming from the degradation of the material, can also be included in h_1.

In a similar way, the consideration of the presence of three groups in DTSG provides the number of functionalities showed in Table 2. The pK_H values obtained; 10.23, 7.6, and 4.52 correlate well with the ones indicated above for the three amino groups in DTPA. As before, the high amount of h_1 groups probably indicates the inclusion of hydroxyl functionalities.

The titration of the algae *S. muticum* was carried out in a previous work (Lodeiro et al., 2008). It demonstrated the presence of two main acid functionalities: carboxyl groups (h_1= 1.78 mmol/g, pK_H= 3.41) and hydroxyl groups (h_1= 1.33 mmol/g, pK_H= 10.2).

FTIR analysis

The quantitative characterization of materials of heterogeneous nature using FTIR technique is a very difficult task. In most of the cases, only semi-qualitative analysis of

the groups present in the surface of the materials can be obtained. Nevertheless, this technique is useful to provide confirmation about the presence or absence of certain chemical groups.

In Figure S4, the FTIR analysis for DTSG before and after some experiments in ASW is shown, together with the spectra for EDSG after the regeneration study.

As expected, Figure S4 shows the main vibrational bands present in SiO_2 spectra (Hamelmann et al., 2005) : 441-450 cm^{-1} (Si-O out of plane deformation), 793 cm^{-1} (Si-O bending), and 1056-1063 cm^{-1} (Si-O-Si stretching and/or C-N stretching of aliphatic amines and/or C-O stretching of alcohols).

The obtained spectra for EDSG (not shown) are almost identical to the obtained for DTSG. Moreover, after the Au reduction, the FTIR spectra did not significantly change, even when Co or Ni were also present. This can be due to the relatively small effect of the gold presence with respect to the great occurrence of other groups, the modification of which was not observed even for initial Au concentrations as high as 2.5 mM (not shown). Nevertheless, when Cr(VI) was also presented in solution and when thiourea was used to remove the gold attached to the EDSG surface, some changes occurred in the structure of these materials as FTIR spectra reveal. Three new bands arose at 697 cm^{-1} (probably due to Si-H and/or N-H wagging), at 2923 cm^{-1} (-CH stretching of hydrocarbon chains), and at 3200-3345 cm^{-1} (stretching of –OH and/or -NH groups). The presence of these bands probably suggests the loss of the functionalization degree of the surface amino groups. In addition, more differences between these materials can be found in the region of the spectra from 1250 to 1800 cm^{-1} (inset of Figure S4).

In this region, amide I, II, and III bands normally arise (Nakamoto, 2009). The peaks at 1604-1635-1638 cm^{-1} can be ascribed to the carbonyl stretching vibrations of the primary amide group introduced after silica gel modification. Moreover, the weak bands

at 1400 cm^{-1} (DTSG and DTSG+Au), 1451-1493 cm^{-1} (DTSG+Au+Cr), and 1396-1460 cm^{-1} (EDSG+thiourea+HCl) arise from the out-of-phase combination of the NH in plane bend and the CN stretching vibrations (amide II).

However, these bands cannot be undoubtedly ascribed to those groups. It is also possible that they correspond to the asymmetric and symmetric stretching of C=O in carboxyl groups, or even to a mixture of bands. In EDTA complexes, un-ionized and un-coordinated COO stretching bands occur at 1700-1750 cm^{-1}, while the ionized and coordinated occur at 1590-1650 cm^{-1}, depending on the nature of the complexed metal (Nakamoto, 2009).

Figure S5 shows the FTIR spectra for the protonated algae *S. muticum* before and after gold retention in ASW. Only a small difference in the position of the band at 621-630 cm^{-1} was observed after the gold reduction by protonated *S. muticum*.

There are some bands in common with respect to the one shown in Figure S5 that arise at 3290 cm^{-1}, 2923, and 1031cm^{-1}. A new weak band at 818 cm^{-1} was assigned to the S=O bond from sulfonate group, normally present in seaweed.

As stated before, the bands from 1250 to 1800 cm^{-1} could correspond to different amide stretching vibrations and/or to symmetric-asymmetric stretching of carboxyl groups. In brown seaweed, typical bands for stretching of O–C–O vibration arise around 1600-1650 (asymmetric) and 1400-1450 (symmetric) cm^{-1} (Lodeiro et al., 2006; Lodeiro et al., 2008; Sheng et al., 2004). Then, the bands showed in Figure S5, 1621-1630 and 1452 cm^{-1}, can also be assigned to the presence of these groups with minor contributions from amide groups. Nevertheless, the band at 1452 cm^{-1} probably arose from stretching vibrations of amide II groups, as mentioned above (Chen and Yang, 2006).

SEM analysis

SEM analysis provides information about the surface microstructure of the materials. Moreover, it allows having an idea about the ions presented, their size or chemical state, which is important to deduce the mechanism for gold recovery. Back-scattered electron images were obtained at different resolutions. Using this technique, the intensity of the signal increases with the atomic number of the elements; so species like Au appear highlighted in the SEM images.

Figure S6 shows the SEM analysis for the EDSG, DTSG, and *S. muticum* materials after kinetic studies for the reduction of Au 0.5 mM. As an example, the RX map for EDSG and the algae is shown, together with the chemical analysis for DTSG, all with a magnification of 8000x.

Figure S6 clearly shows the presence of Au over the surface of the materials. The brilliant particles in the SEM images correspond to Au as the RX map confirms. In the map pictures, where the position and identification of the different elements present is shown, it is clearly stated that the main components in EDSG are C, Si, and O, as expected. The presence of Na and Cl, the main ions in ASW, was also evidenced. The Figure S6b showed the qualitative analysis of the elements found in the corresponding SEM image. The percentage of Au found is clearly highlighted after the main components are present in DTSG material.

The particle distribution shown in the SEM pictures reveals the presence of gold with different morphologies and sizes (Figures S6 and 7).

Most of the gold particles have spherical or amorphous shapes ranging from 100 to 500 nm or even higher in some particle aggregations. Nevertheless, when gold was attached over the EDSG or DTSG surface, also particles with hexagonal or triangular forms (300-1500 nm side) can be found, together with nanowires with the width of around 50-

250 nm. Probably, the spherical particles act as seeds over which the deposition of gold occurs.

SEM images were also obtained for Cr(VI) and Co competition in gold retention over DTSG surface. As expected, the EDS analysis of the images reveals the presence of these metals. Figure 7 shows an example of the Cr (5mM) and Au (0.5 mM) competition, in which the main elements present in the ASW were found (Figure S7) together with Au (0.61 % atomic) and Cr (0.15 % atomic).

All these particles are really stable. After being stored for several months in plastic recipients they did not undergo degradation, preserving their physical and chemical properties.

SEM images obtained after the regeneration experiments with thiourea and DTSG (120 hours of contact time) showed no presence of Au particles over the surface of the materials (pictures not shown).

It is worth mentioning that using this SEM under the mentioned conditions it is difficult to detect particles whose diameter is less than 40 nm.

4. CONCLUSIONS

Based on the results showed above it can be concluded that the gold removal from artificial seawater is mainly an adsorption coupled reduction mechanism. The following steps in the mechanism are proposed:

1. Adsorption of the anion species $AuCl_4^-$, present in artificial seawater solution with a pH lower than 4, due to the formation of an ion pair with the protonated amino and hydroxyl groups present on the surface of the materials.

This was confirmed by the lack of pH dependence found in the experiments, which implies that the groups involved in gold attraction are protonated in the pH interval

studied. Additional confirmation arises from the absence of the color change on the surface of the materials during the first stage of the kinetic experiments.

2. Reduction of the $AuCl_4^-$ to $AuCl_2^-$, probably due to the dissolution of some metallic gold favored by the high chloride concentration in solution (Marsden and House, 2006), according to the following reactions:

$$AuCl_4^- + 3e^- \leftrightarrow Au(s) + 4Cl^- \qquad E_1^0 = +1.002\ V$$

$$-(3AuCl_2^- + 3e^- \leftrightarrow 3Au(s) + 6Cl^-) \qquad E_2^0 = -1.154\ V$$

$$2Au(s) + 2Cl^- + AuCl_4^- \leftrightarrow 3AuCl_2^- \qquad E_t^0 = E_1^0 - E_2^0 = +2.156\ V$$

The formed $AuCl_2^-$ species is not stable in solution and can be oxidized further to Au(III):

$$AuCl_2^- + 2Cl^- \leftrightarrow AuCl_4^- + 2e^-$$

The increase in the gold concentration detected during the second stage in kinetic experiments provides an additional confirmation for the equations proposed above. Here it is stated that some chloro-gold complex previously adsorbed or some metallic gold return to the solution in the form of unstable $AuCl_2^-$ species. Moreover, at the end of the second kinetic stage, the material started to change the color from white-brown to purple-black, indicating the formation of gold nanoparticles.

3. Reduction of the chloro-gold complexes to metallic gold. This corresponds with the last stage in the kinetics where an exponential decay of gold concentration in solution was observed. During this step, the oxidation of the hydroxyl and amino groups is more intense, producing a continuous formation of reduced gold on the surface of the materials. The following general reactions are proposed:

$$AuCl_4^- + 3e^- \leftrightarrow Au(s) + 4Cl^-$$

$$R - OH \leftrightarrow R = O + H^+ + e^-$$

$$R_3N^- - H + H_2O \leftrightarrow R_3N^+ - OH + 2H^+ + 2e^-$$

During this step, a continuous color change was observed from purple-black to black, more and more intense, confirming again the formation of gold nanoparticles. This was also supported by the SEM studies.

ACKNOWLEDGEMENTS

P. Lodeiro gratefully acknowledges the financial support through Ángeles Alvariño projects AA 10.02.56B.444.0 and 09.02.561B.444.0 (Xunta de Galicia), both co-funded with 80 % by European Social Funds.

REFERENCES

Carro, L. et al., 2010. A dynamic proof of mercury elimination from solution through a combined sorption-reduction process. Bioresource Technology, 101: 8969-8974.

Castro, L. et al., 2011. Biosynthesis of gold nanowires using sugar beet pulp. Process Biochemistry, 46: 1076-1081.

Chen, J.P. and Yang, L., 2006. Study of a heavy metal biosorption onto raw and chemically modified *Sargassum* sp. via spectroscopic and modeling analysis. Langmuir, 22: 8906-8914.

Choma, J., Dziura, A., Jamiola, D., Nyga, P. and Jaroniec, M., 2011. Preparation and properties of silica–gold core–shell particles. Colloids and Surfaces A-Physicochemical And Engineering Aspects, 373: 167-170.

Davis, T.A., Volesky, B. and Mucci, A., 2003. A review of the biochemistry of heavy metal biosorption by brown algae. Water Research, 37(18): 4311-4330.

Dubey, S.P., Lahtinen, M. and Sillanpää, M.E.T., 2010. Green synthesis and characterizations of silver and gold nanoparticles using leaf extract of *Rosa rugosa*. Colloids and Surfaces A-Physicochemical And Engineering Aspects, 364: 34-40.

Falkner, K.K. and Edmond, J.M., 1990. Gold in seawater. Earth and Planetary Science Letters, 98(2): 208-221.

Figueira, M.M., Volesky, B., Ciminelli, V.S.T. and Roddick, F.A., 2000. Biosorption of metals in brown seaweed biomass. Water Research, 34(1): 196-204.

Guo, S. and Wang, E., 2007. Synthesis and electrochemical applications of gold nanoparticles. Analytica Chimica Acta, 598: 181-190.

Hamelmann, F., Heinzmann, U., Szekeres, A., Kirov, N. and Nikolova, T., 2005. Deposition of silicon oxide thin films in teos with addition of oxygen to the

plasma ambient: IR spectra analysis. Journal of Optoelectronics and Advanced Materials, 7(1): 389-393.

Herrero, R. et al., 2011. Full description of copper uptake by algal biomass combining an equilibrium NICA model with a kinetic intraparticle diffusion driving force approach. Bioresource Technology, 102: 2990-2997.

Johnston, J.H. and Lucas, K.A., 2011. Nanogold synthesis in wool fibres: novel colourants. Gold Bulletin, 44: 85-88.

Katchalsky, A., Shavit, N. and Eisenberg, H., 1954. Dissociation of weak polymeric acids and bases. Journal of Polymer Science, 13: 69-84.

Kavakli, C., Malci, S., Tuncel, S.A. and Salih, B., 2006. Selective adsorption and recovery of precious metal ions from geological samples by 1,5,9,13-tetrathiacyclohexadecane-3,11-diol anchored poly(p-CMS-DVB) microbeads. Reactive & Functional Polymers, 66: 275-285.

Koide, M., Hodge, V. and Goldberg, E.D., 1988. Gold in seawater: a conservative view. Applied Geochemistry, 3(3): 237-241.

Layton, V.W. and Mueller, E., 1981. Process for the continuous recovery of gold and other metals from sea water. In: U.S. Patent (Editor), U.S. Patent, United States.

Lodeiro, P., Barriada, J.L., Herrero, R. and Sastre de Vicente, M.E., 2006. The marine macroalga *Cystoseira baccata* as biosorbent for cadmium (II) and lead (II) removal: kinetic and equilibrium studies. Environmental Pollution, 142: 264-273.

Lodeiro, P., Fuentes, A., Herrero, R. and Sastre de Vicente, M.E., 2008. Cr^{III} binding by surface polymers in natural biomass: the role of carboxylic groups. Environmental Chemistry, 5: 355-365.

Lodeiro, P., Gudiña, A., Herrero, L., Herrero, R. and Sastre de Vicente, M.E., 2010. Aluminium removal from wastewater by refused beach cast seaweed. Equilibrium and dynamic studies. Journal of Hazardous Materials, 178: 861-866.

López-García, M., Lodeiro, P., Barriada, J.L., Herrero, R. and Sastre de Vicente, M.E., 2010. Reduction of Cr(VI) levels in solution using bracken fern biomass: Batch and column studies. Chemical Engineering Journal, 165: 517-523.

Marsden, J.O. and House, L., 2006. The Chemistry of Gold Extraction, Colorado, USA, 655 pp.

Mata, Y.N. et al., 2009. Gold(III) biosorption and bioreduction with the brown alga *Fucus vesiculosus*. Journal of Hazardous Materials, 166: 612-618.

Millero, F.J., 1986. The pH of estuarine waters. Limnology and Oceanography, 31(4): 839-847.

Montes, M.O. et al., 2011. Anisotropic gold nanoparticles and gold plates biosynthesis using alfalfa extracts. Journal of Nanoparticle Research, 13(8): 3113-3121.

Nakamoto, K., 2009. Infrared and Raman Spectra of Inorganic and Coordination Compounds. Part B, Part B. John Wiley & Sons, Inc., United States, 408 pp.

Nilanjana, D., 2010. Recovery of precious metals through biosorption — A review. Hydrometallurgy, 103: 180-189.

Puigdomenech, I., 1999. MEDUSA and HYDRA software for chemical equilibrium calculations, version 19. Royal Institute of Technology, Stochholm, Sweden.

Rämö, J. and Sillanpää, M., 2001. Degradation of EDTA by Hydrogen Peroxide in Alkaline Conditions. Journal of Cleaner Production, 9: 191-195.

Rämö, J., Sillanpää, M., Vickackaite, V., Orama, M. and Niinistö, L., 2000. Chelating Ability and Solubility of DTPA, EDTA and β-ADA in Alkaline Hydrogen Peroxide Environment. Journal of Pulp and Paper Science, 26: 125-131.

Repo, E., Kurniawan, T.A., Warchol, J.K. and Sillanpaa, M.E.T., 2009. Removal of Co(II) and Ni(II) ions from contaminated water using silica gel functionalized with EDTA and/or DTPA as chelating agents. Journal of Hazardous Materials, 171(1-3): 1071-1080.

Repo, E., Malinen, L., Koivula, R., Harjula, R. and Sillanpaa, M., 2011. Capture of Co(II) from its aqueous EDTA-chelate by DTPA-modified silica gel and chitosan. Journal of Hazardous Materials, 187(1-3): 122-132.

Rey-Castro, C., Herrero, R. and de Vicente, M.E.S., 2004. Gibbs-Donnan and specific-ion interaction theory descriptions of the effect of ionic strength on proton dissociation of alginic acid. Journal of Electroanalytical Chemistry, 564(1-2): 223-230.

Rey-Castro, C., Lodeiro, P., Herrero, R. and Sastre de Vicente, M.E., 2003. Acid-base properties of brown seaweed biomass considered as a Donnan Gel. A model reflecting electrostatic effects and chemical heterogeneity. Environmental Science & Technology, 37(22): 5159-5167.

Saha, K., Agasti, S.S., Kim, C., Li, X. and Rotello, V.M., 2012. Gold Nanoparticles in Chemical and Biological Sensing. Chemical Reviews, 112: 2739-2779.

Sheng, P.X., Ting, Y.P., Chen, J.P. and Hong, L., 2004. Sorption of lead, copper, cadmium, zinc and nickel by marine algal biomass: characterization of biosorptive capacity and investigation of mechanisms. Journal of Colloid and Interface Science, 275: 131-141.

Sillanpää, M., 1996. Complexing Agents in Waste Water Effluents of three Finnish Pulp and Paper Mills. Chemosphere, 33: 293-302.

Sillanpää, M., Kokkonen, R. and Sihvonen, M.L., 1995. Determination of EDTA and DTPA as their Fe(III) Complexes in Pulp and Paper Mill Process and Waste Waters by Liquid Chromatography. Analytica Chimica Acta, 303: 187-192.

Sillanpää, M. and Pirkanniemi, K., 2001. Recent Developments in Chelate Degradation. Environmental Technology, 22: 791-801.

Sillanpää, M. and Sihvonen, M.L., 1997. Analysis of EDTA and DTPA. Talanta, 44: 1487-1497.

Smith, R.M., Martell, A.E. and Motekaitis, R.J., 2007. NIST standard reference database 46.6, Deparment of Commerce, Gaithersburg, MD.

Sreeprasad, T.S. and Pradeep, T., 2011. Reversible Assembly and Disassembly of Gold Nanorods Induced by EDTA and Its Application in SERS Tuning. Langmuir, 27: 3381-3390.

Syed, S., 2012. Recovery of gold from secondary sources—A review. Hydrometallurgy, 115-116: 30-51.

TABLES

Table 1. Gold removal percentage at different doses and times of EDSG and DTSG. The initial gold concentration was 0.25 mM.

	EDSG		DTSG	
Dose g/L	27 h %	161 h %	27 h %	161 h %
0.1	45.7	46.4	45.3	39.7
0.5	67.1	97.6	89.9	98.3
1	91.3	99.5	97.1	99.8
2	95.6	98.9	98.7	99.5
4	97.2	98.8	99.5	99.1

Table 2. Adjustable parameters obtained from the fit of Equation 4 to the titration curves of the selected materials. h is expressed in mmol/g. Errors are shown in brackets.

	2 groups				**3 groups**					
	h_1	pK_{H1}	h_2	pK_{H2}	h_1	pK_{H1}	h_2	pK_{H2}	h_3	pK_{H3}
EDSG	2.20 (0.05)	10.04 (0.03)	0.34 (0.02)	4.9 (0.4)	2.22 (0.02)	10.11 (0.01)	0.21 (0.01)	7.2 (0.1)	0.20 (0.01)	4.0 (0.1)
r^2	0.995				0.9996					
DTSG	2.44 (0.06)	10.15 (0.02)	0.30 (0.01)	5.4 (0.3)	2.50 (0.02)	10.23 (0.01)	0.18 (0.01)	7.6 (0.1)	0.19 (0.01)	4.52 (0.05)
r^2	0.997				0.99990					

FIGURE CAPTIONS

Figure 1 Kinetic of EDSG for Au recovery from ASW at different initial metal concentrations: 0.05 mM (squares) and 0.5 mM (circles). The inset represents the evolution of pH and E_{redox} during the experiments (Au 0.5 mM)

Figure 2 Kinetic of DTSG for Au recovery from ASW at different initial metal concentrations: Au 0.25 mM (diamonds) and 0.5 mM (circles). The inset represents the evolution of pH and E_{redox} during the experiments (Au 0.5 mM)

Figure 3 Kinetic of protonated S. muticum for Au recovery from ASW at 0.5 mM initial metal concentration. The inset represents the evolution of pH and E_{redox} during the experiments

Figure 4 a) Effect of the presence of Co at different initial concentrations over gold recovery (0.5 mM). Dose 4 g/L. pH= 3.1, 3.2, and 2.6. b) Effect of the presence of Ni at different initial concentrations over gold recovery (0.5 mM). Dose 4 g/L. pH= 3.1, 3.1, and 2.6

Figure 5 Effect of the presence of Cr(VI) at different initial concentrations over gold recovery (0.5 mM). Dose 4 g/L. pH= 3.2, 3.1, and 2.7

Figure 6 Breakthrough curves for gold recovery in artificial seawater at different flow rates: 5 mL/min (white symbols) and 1mL/min (grey symbols), and EDSG quantities: 0.05 (circles), 0.1 (squares), and 0.2 g (triangles)

Figure 7 SEM image of DTSG surface at a magnification of 10000x, after the experiment of Cr(VI) 5mM and Au 0.5 mM competition. The arrows mark the brilliant shapes representing gold particles.

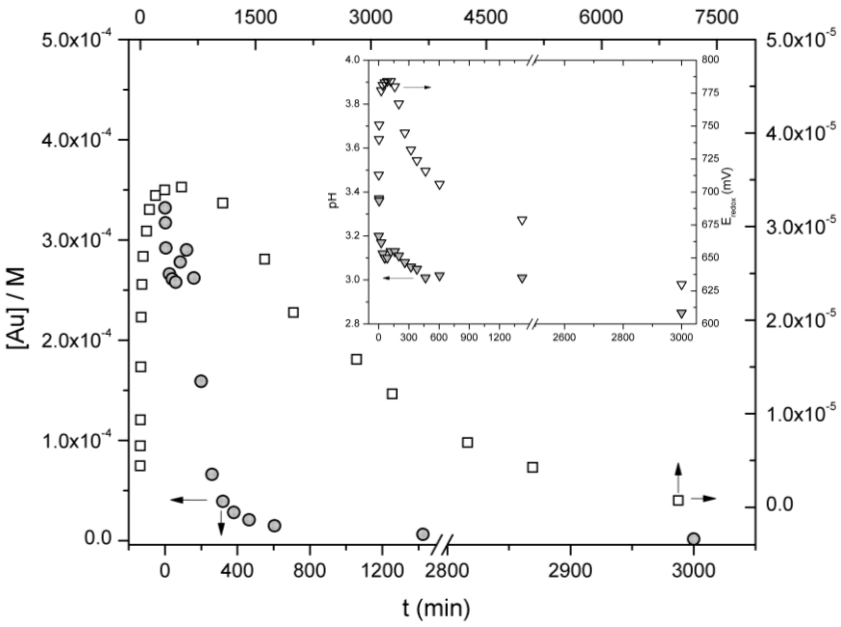

Figure 1

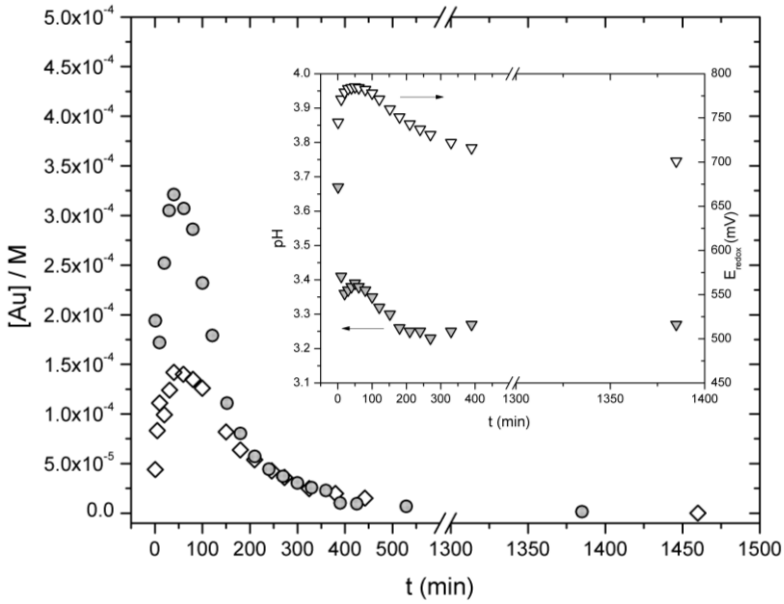

Figure 2

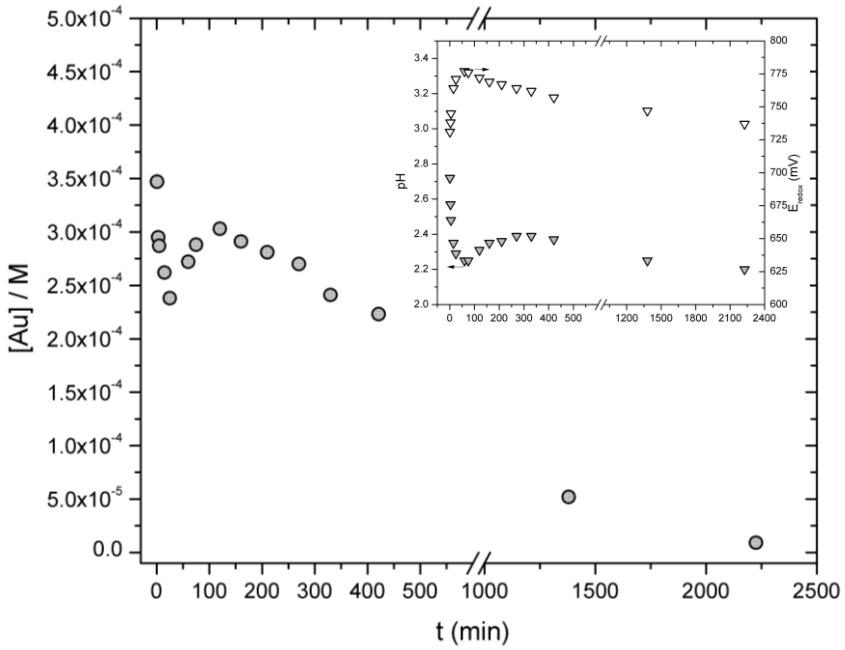

Figure 3

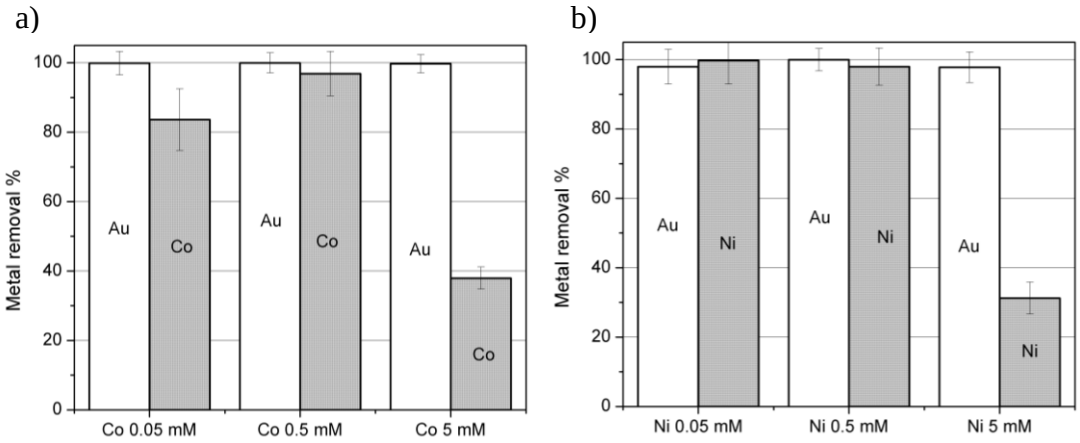

Figure 4

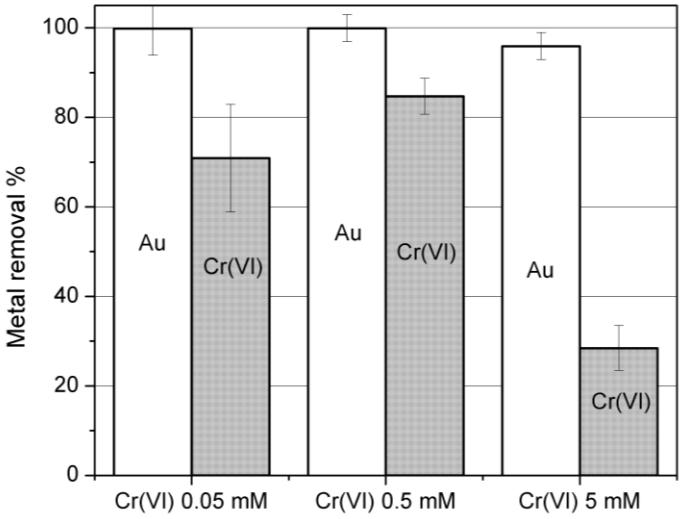

Figure 5

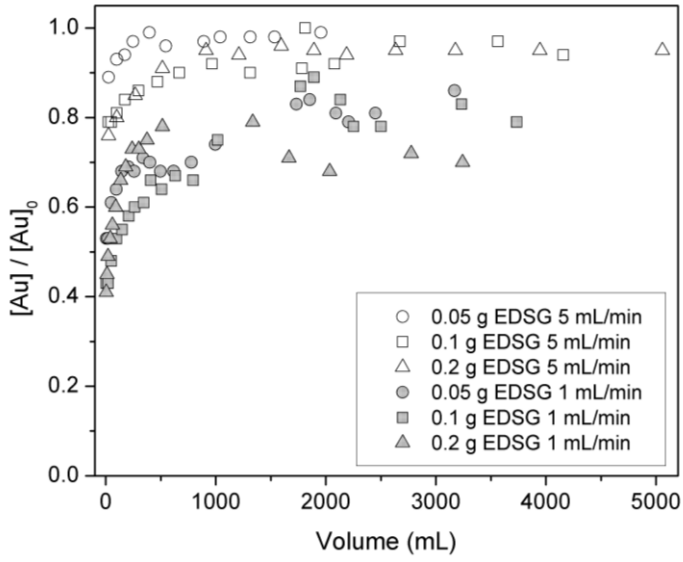

Figure 6

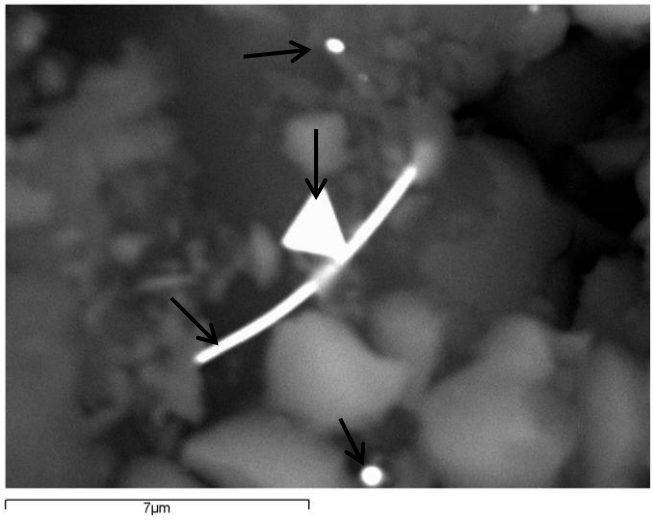

Figure 7

Electronic Supplementary Material available

ELECTRONIC SUPPLEMENTARY MATERIAL FOR:

Gold Recovery From Artificial Seawater Using Synthetic Materials And Seaweed Biomass To Induce Gold Nanoparticles Formation In Batch And Column Experiments

Pablo Lodeiro[1*] and Mika Sillanpää[2]

[1]Department of Physical Chemistry and Chemical Engineering I, University of A Coruña, Rúa da Fraga 10, 15008 A Coruña, Spain.

[2]Laboratory of Green Chemistry, Department of Energy and Environmental Technology, Faculty of Technology, Lappeenranta University of Technology, Finland.

*Corresponding author e-mail address: plodeiro@udc.es; Tel.: (+34) 981 167000 (ext. 2199); Fax: (+34) 981 167065

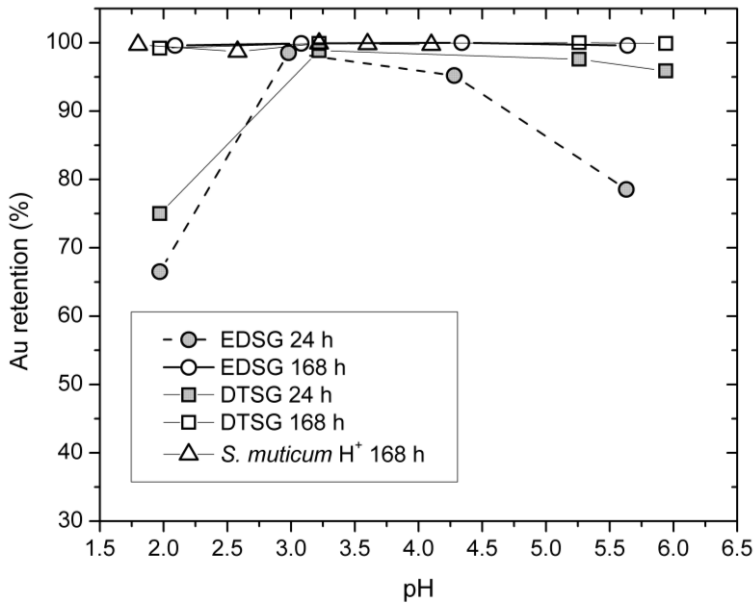

Figure S1. *Effect of pH over gold recovery from artificial seawater at different times. Gold initial concentration 0.5 mM, dose of 4 g/L.*

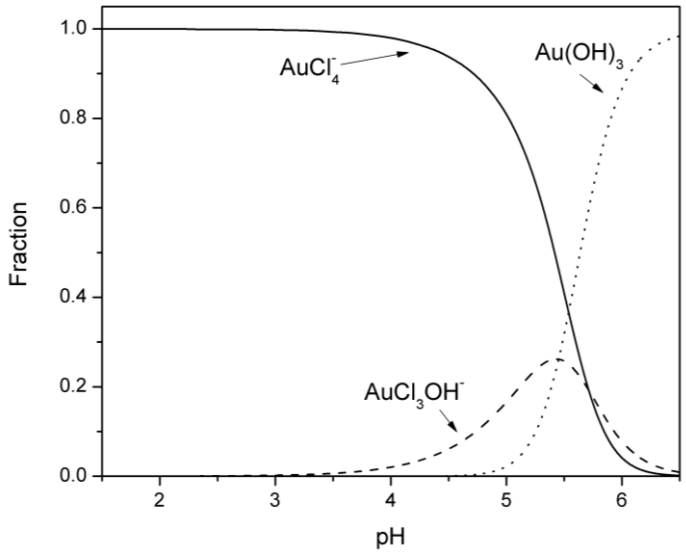

Figure S2. *Speciation diagram as a function of pH for $HAuCl_4$ 0.5 mM in ASW.*

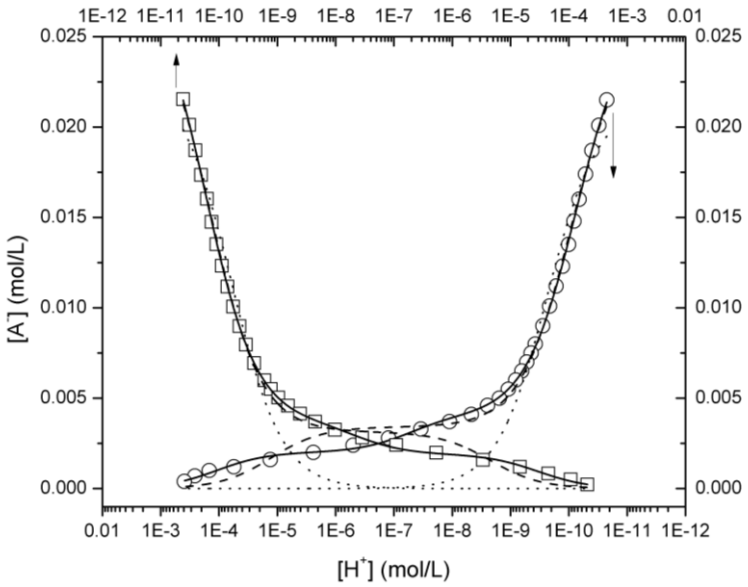

Figure S3. *Potentiometric titrations of EDSG (circles) and DTSG (squares). The lines represent the fit to Equation 4, taking into consideration one (dotted line), two (dashed line), or three (solid line) functional groups.*

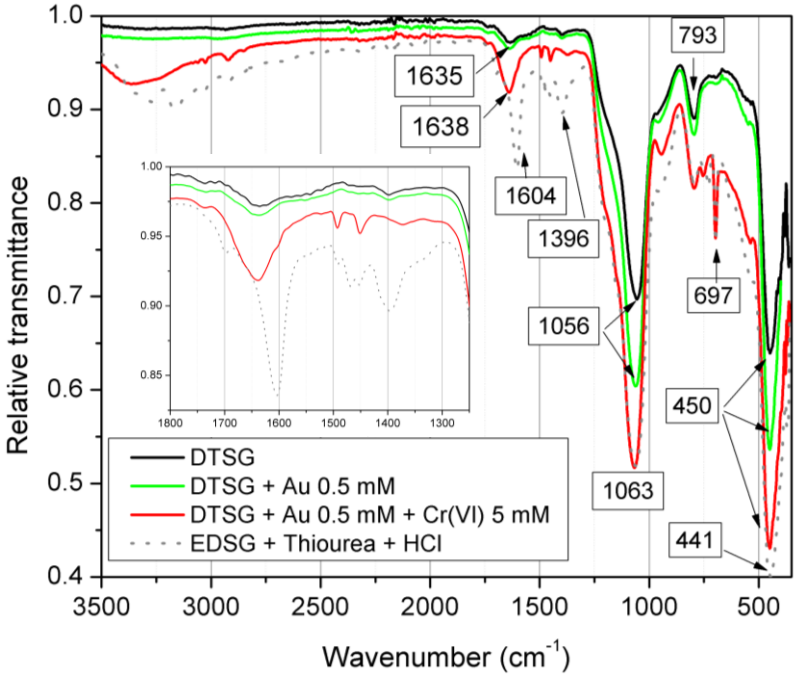

Figure S4. *FTIR spectra for DTSG (black line), DTSG + Au 0.5 mM in ASW after 71 hours of contact (green line), DTSG + Au 0.5 mM + Cr(VI) in ASW after 96 hours of contact (red line), and EDSG containing gold + thiourea + HCl 1M after 120 hours of contact (grey dashed line).*

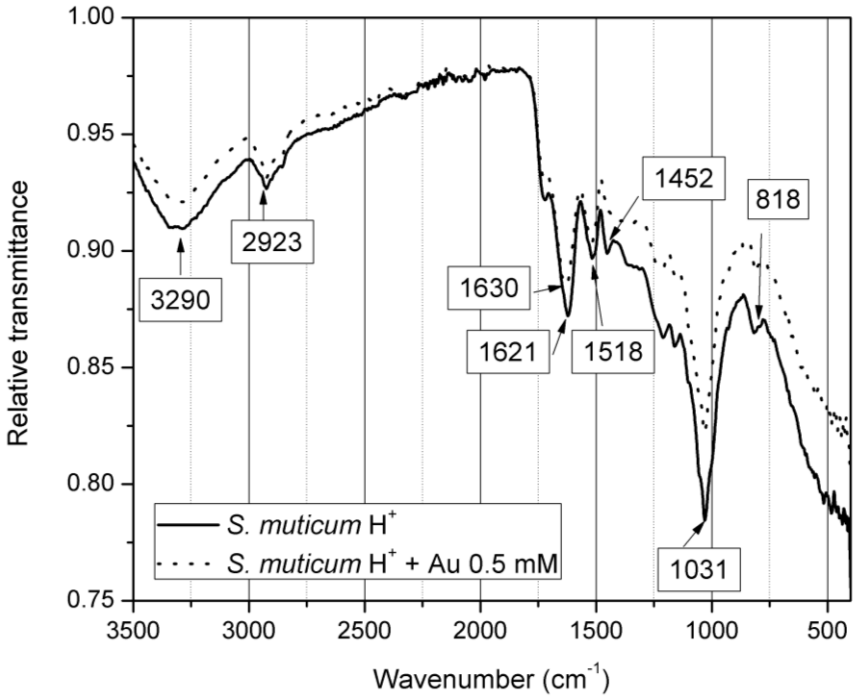

Figure S5. *FTIR spectra for protonated S. muticum (black line) and S. muticum + Au 0.5 mM in ASW after 37 hours of contact (black dashed line).*

a)

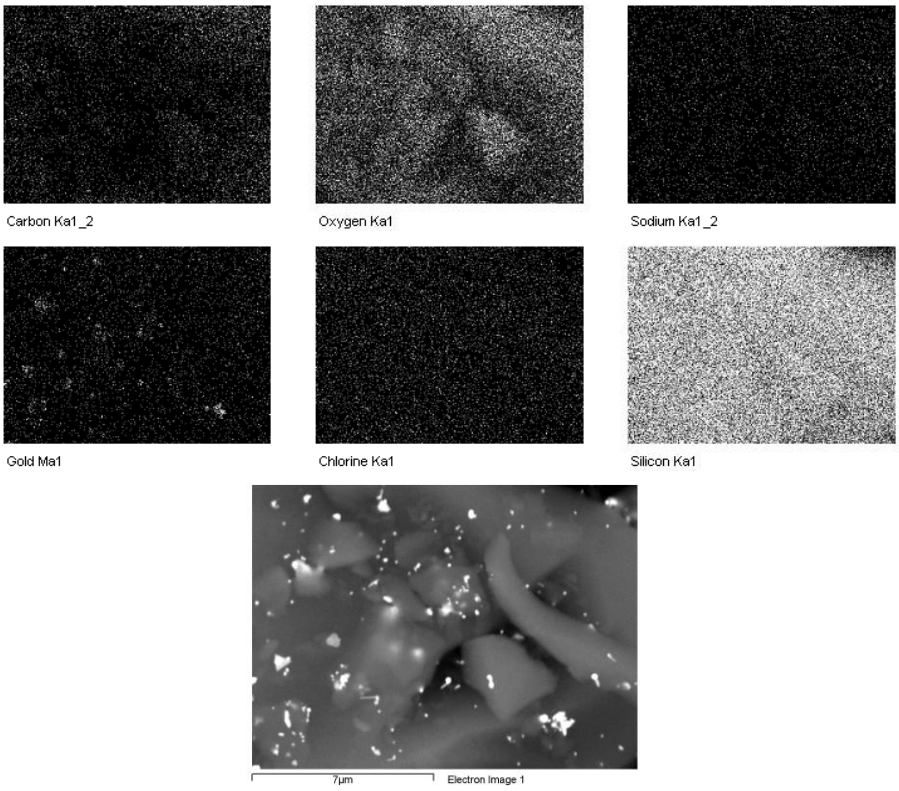

b)

Element	C	O	Si	Cl	Cu	Zn	Au	Totals
Weight (%)	27.22	19.13	27.02	0.46	2.37	2.09	21.70	100.00
Atomic (%)	49.09	25.90	20.84	0.28	0.81	0.69	2.39	100.00

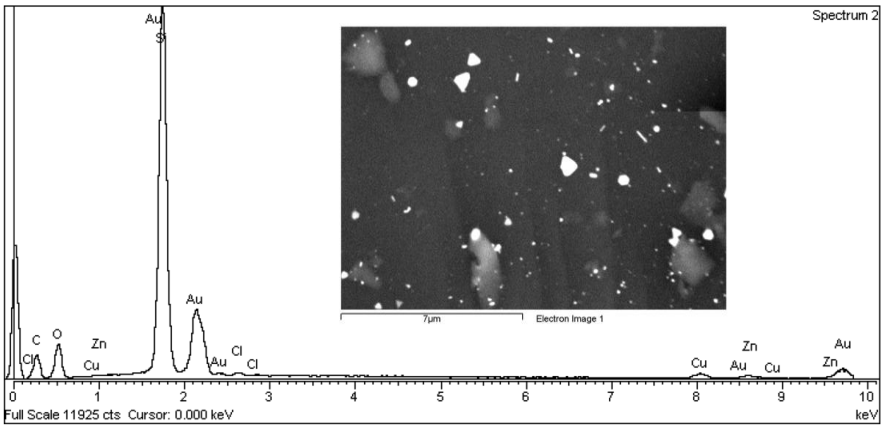

c)

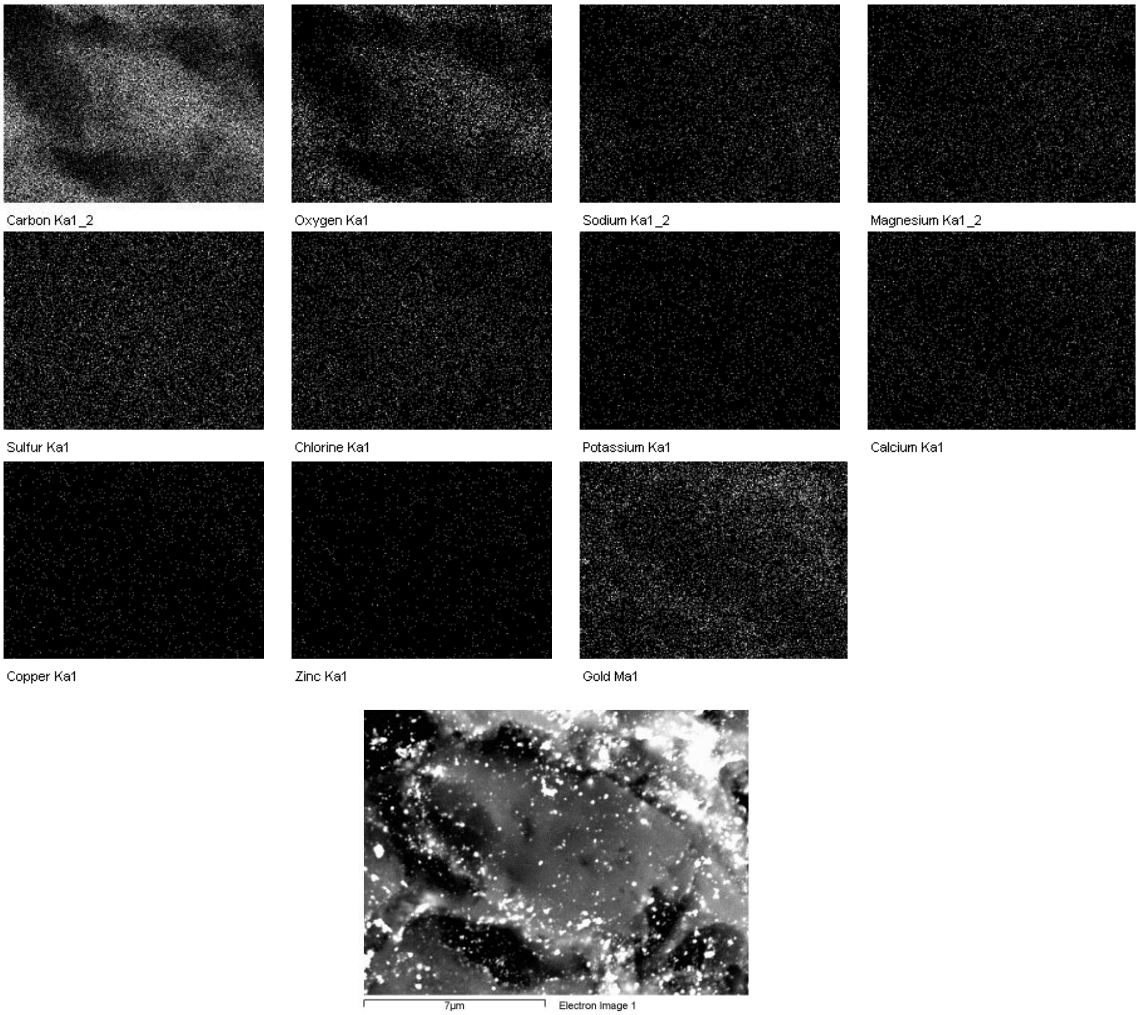

Figure S6. *a) RX map of EDSG after contact (50 hours) with Au 0.5 mM in ASW. b) Qualitative analysis of the elements present on the surface of DTSG after contact (71 hours) with Au 0.5 mM in ASW. c) RX map of S. muticum after contact (37 hours) with Au 0.5 mM in ASW.*

Element	C	O	Si	Cl	Cr	Mg	Cu	F	Au	Totals
Weight (%)	57.50	19.85	6.62	2.40	0.51	0.53	0.98	2.58	7.87	100
Atomic (%)	72.75	18.85	3.58	1.03	0.15	0.33	0.24	2.07	0.61	100

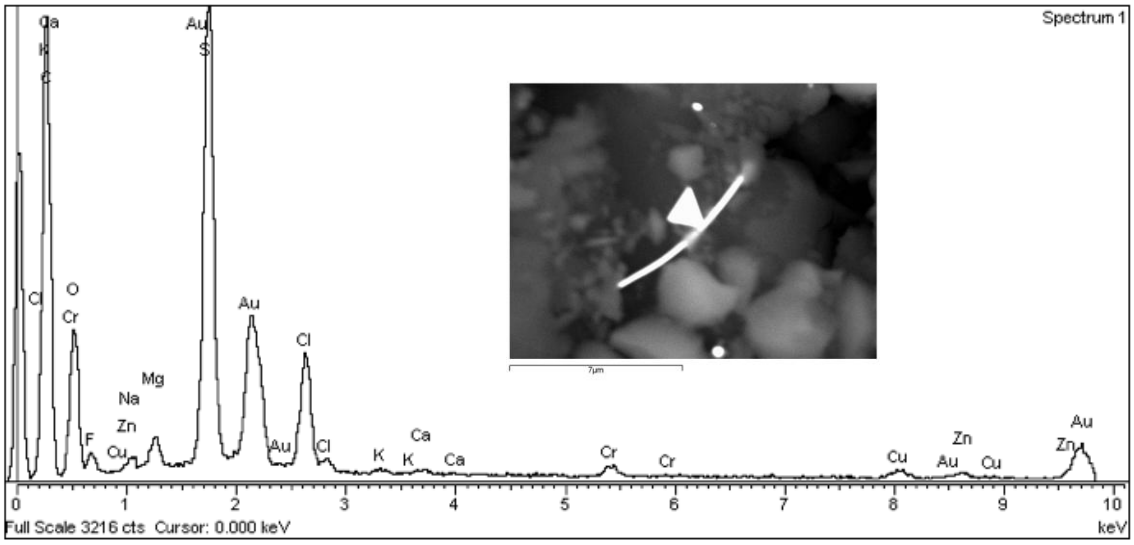

Figure S7. *Qualitative analysis of the elements present on the surface of DTSG after the experiment of Cr(VI) 5mM and Au 0.5 mM competition in ASW.*

***Research Highlights**

- Gold recovery from artificial seawater through nanoparticle formation
- No effect of pH or presence of other metal over gold recovery
- A plausible three-step mechanism was suggested for the adsorption-reduction process
- Titrations, FTIR and SEM provided decisive evidence supporting the mechanism

GRAPHICAL ABSTRACT

Gold nanoparticles formation in silica gel-DTPA material, after the recovery of Au from artificial seawater. From left to right: total recovery of 0.05, 0.25, 0.5 and 2.5 mM Au from artificial seawater.